HEPATOBILIARY-PANCREAS

Emilio Quaia
Valerio Alaimo
Elisa Baratella
Alessandro Medeot
Massimo Midiri
Maria Assunta Cova

The added diagnostic value of 64-row multidetector CT combined with contrast-enhanced US in the evaluation of hepatocellular nodule vascularity: implications in the diagnosis of malignancy in patients with liver cirrhosis

E. Quaia (✉) · E. Baratella ·
A. Medeot · M. A. Cova
Department of Radiology,
Cattinara Hospital,
University of Trieste,
Strada di Fiume 447,
34149 Trieste, Italy
e-mail: equaia@yahoo.com
Tel.: +39-40-3994372
Fax: +39-40-3994500

V. Alaimo · M. Midiri
Department of Radiology,
University of Palermo,
Via Del Vespro 127,
90127 Palermo, Italy

Abstract The aim of this study was to assess the added diagnostic value of contrast-enhanced US (CEUS) combined with 64-row multidetector CT (CT) in the assessment of hepatocellular nodule vascularity in patients with liver cirrhosis. One hundred and six cirrhotic patients (68 male, 38 female; mean age ± SD, 70±7 years) with 121 biopsy-proven hepatocellular nodules (72 hepatocellular carcinomas, 10 dysplastic and 15 regenerative nodules, 12 hemangiomas, and 12 other benignancies) detected during US surveillance were prospectively recruited. Each nodule was scanned by CEUS during the arterial (10–40 s), portal venous (45–90 s), and delayed sinusoidal phase (from 100 s after microbubble injection to microbubble disappearance). Nodule vascularity at CEUS, CT, and combined CEUS/CT was evaluated side-by-side by two independent blinded readers who classified nodules as benign or malignant according to reference diagnostic criteria. The combined assessment of CEUS/CT provided higher sensitivity (97%, both readers) than did separate assessment of CEUS (88% reader 1; 87% reader 2) and CT (74% reader 1; 71% reader 2; P<0.05), while no change in specificity was provided by combined analysis. The combined assessment of hepatocellular nodule vascularity at CT and CEUS improved sensitivity in the diagnosis of malignancy in patients with liver cirrhosis.

Keywords Ultrasound ·
Liver cirrhosis · Hepatocellular carcinoma · Microbubble contrast agents

Introduction

One of the key pathological factors for the differential diagnosis between hepatocellular carcinoma (HCC) and non-malignant hepatocellular lesions in cirrhotic patients is the vascular supply to the nodule [1–3]. Both contrast-enhanced computed tomography (CT) and magnetic resonance (MR) imaging are considered reliable techniques for depicting hepatocellular nodule vascularity in the non-invasive diagnosis of hepatocellular nodules in the cirrhotic patient. According to the 2001 Barcelona criteria [2, 3], evidence of coincidental arterial hypervascularity at contrast-enhanced CT and MR imaging in nodules >2 cm in patients with liver cirrhosis is considered diagnostic of

HCC, and no bioptic procedure is required [2, 3]. If a nodule >2 cm shows arterial hypervascularity and washes out in the early or delayed venous phase, only a single imaging investigation (contrast-enhanced CT or MR) is required for HCC diagnosis [3]. If an equivocal pattern is identified (e.g., iso- or hypervascularity not followed by hypovascularity, or persistent hypovascularity) in nodules of any size either follow-up imaging for rapid progression or biopsy for confirmation should be performed [2, 3]. Mulidetector computed tomography (CT) after the intravenous bolus injection of iodinated contrast agents currently plays a fundamental role in the diagnosis of HCC [4–7] as a result of the marked reduction in the time required for thin-section imaging of the entire liver relative

to standard single-detector spiral CT. Contrast-enhanced ultrasound (CEUS) may also reliably depict arterial hypervascularity in the majority of hepatocellular nodules and particularly in HCCs [8–12]. It was also recently shown that CEUS presents a high level of concordance with CT [13–16] and MR imaging [16, 17] in depicting the enhancement pattern of focal liver lesions during the arterial phase. To our knowledge, no previous study has extensively analyzed the potential synergic diagnostic capabilities of CEUS combined with 64-row multidetector CT in the evaluation of hepatocellular nodule vascularity in the cirrhotic patients.

The aim of this study was to assess the added diagnostic value of CEUS combined with 64-row multidetector CT in the assessment of hepatocellular nodule vascularity in patients with liver cirrhosis.

Subjects and methods

Patients

This was a prospective open-label study. Approval was obtained from the ethics committees (equivalent to the Institutional Review Board) of the two participating hospitals, and informed consent was obtained from all patients at the time of scanning after the nature of the procedure had been fully explained.

One hundred eighty cirrhotic patients (120 male, 60 female; mean age ± SD, 71±7 years) who had at least one hepatocellular nodule identified during US surveillance were prospectively recruited. All patients had a definite diagnosis of liver cirrhosis (Child-Turcotte-Pugh class A or B) related to viral infection [hepatitis B (n=85 patients),

hepatitis C (n=52), or both (n=3)], or alcohol abuse (n=40), obtained by means of biopsy or unequivocal imaging findings including irregular liver margins and nodulations. From 1 to 20 days after identification of the nodule(s), up to two nodules per patient, for a total number of 195 hepatocellular nodules were selected for CEUS on the basis of largest diameter and best visualization through the acoustic window. All nodules were examined by contrast-enhanced 64-row multidetector CT of the liver from 2 to 30 days after CEUS. In this study we included only those nodules ≤3 cm in diameter that underwent biopsy after CT corresponding to nodules that were not characterized based on the Barcelona criteria [2, 3] (nodule ≤ or >2 cm in diameter with hypervascularity during the arterial phase without hypovascularity in the portal venous phase, or nodules with isovascularity during the arterial phase and hypovascularity during the portal phase, or nodules with persistent hypovascularity during all dynamic phases). Those hepatocellular nodules revealing peripheral nodular enhancement (discontinuous or continuous peripheral nodular appearance) at contrast-enhanced CT were excluded from the study due to the high probability of hemangioma diagnosis.

Two reference radiologists, affiliated to the two hospitals involved in the study, excluded 74 nodules in 74 patients because of lack of a histologic diagnosis (n=60), technical inadequacy of CT (n=10; incorrect time delay for the arterial phase scanning), or CEUS examination (n=4; failure in data storage or incomplete nodule visibility).

Therefore, the final study group consisted of 106 patients (mean age ± SD, 70±7 years), including 68 men (mean age ± SD, 62±11; median age, 64; range 29–84 years) and 38 women (mean age ± SD, 60±9; median age, 60; range 30–75 years) with 121 hepatocellular nodules (Table 1).

Table 1 General features of the hepatocellular nodule histotypes

Histotypes	Number	Mean size ± SD (cm)	Dimension range (cm)	≤2 cm	>2 cm
Hepatocellular carcinomas	72 *	2.1±0.9	1 – 3	41	31
Dysplastic nodules	10 ◊	1.9±0.6	1 – 3	9	1
Regenerative nodules	15	1.9±0.8	1 – 3	12	3
Hemangiomas	12 ‡	1.9±0.7	1 – 3	11	1
Other benign histotypes	3 ♦	1.9±0.7	1 – 3	1	2
Pseudotumors	9 §	1.7±0.6	1 – 3	8	1
Total	121	1.9±1.1	1 – 3	82	39

Diagnostic features of each hepatocellular nodule histotype
*Nodules included 46 well-differentiated and 26 moderately or poorly differentiated hepatocellular carcinomas
◊Dysplastic nodules revealed a low- (n=7) or high-grade (n=3) pattern
‡Liver hemangiomas revealed a hypervascular (n=7) or thrombotic-fibrotic (n=2) pattern at histology. The remaining hemangiomas (n=3) revealed endothelial-lined vascular channels
♦This diagnostic category included one necrotic nodule (1.5 cm), one focal nodular hyperplasia (3 cm), and one hepatocellular adenoma (3 cm)
§Pseudotumors included intrahepatic arterio-portal non-tumorous shunts (n=5), focal fibrosis (n=2), and focal fatty infiltration (n=2)

Contrast-enhanced US examination

The US examinations considered in the present series were performed by board-certified diagnostic radiologists affiliated with the two hospitals involved in the study and with at least 5 years of experience in liver US imaging. For consistency the two centers used the same state-of-the-art US equipment (Sequoia, Acuson, Siemens, Mountain View, CA; convex array 2–4 MHz 4C1 transducer) and the same ultrasound protocol, consisting of a preliminary gray-scale and color or power Doppler unenhanced US scan followed by CEUS.

The largest diameter of the nodule was measured in the transverse or longitudinal plane at unenhanced US, and the nodule was located in a liver segment according to the Couinaud and Bismuth classification systems [18, 19]. Tumor vessels were imaged at low-flow settings (pulse repetition frequencies 800–1,500 Hz, wall filter of 40–50 Hz, high levels of color versus echo priority and color persistence) and Doppler spectral analysis of peripheral and intranodular vessels. Sulfur hexafluoride-filled microbubbles were then manually injected as a 2.4-ml bolus through an 18–20-gauge i.v. cannula and followed by a 10-ml normal saline flush. Each nodule was examined by using real-time continuous insonation during normal breathing or breath-holding, depending on which yielded the best visualization of the nodule. The arterial phase was timed 10-40 s after microbubble injection, the portal venous phase from 45–90 s, and the delayed sinusoidal phase from 100 s up to microbubble disappearance.

Technical parameters were: cadence contrast pulse sequencing as a contrast-specific technique, low transmit power (mechanical index: 0.09-0.14), dynamic range 65 dB, temporal resolution between frames 75–100 ms (10-13 frames per second), echo-signal gain below noise visibility, and one focus below the level of the tumor. Distinct digital cine-clips for the unenhanced US scan and for the arterial, portal venous, and delayed phase of the CEUS scan were stored on a PC (Intel, Pentium 4, Santa Clara, CA) connected to the US equipment by a high-performance hardware-based real-time Moving Picture Experts Group-2 (MPEG-2) encoder (MVR1000, Mediacruise, Canopus Corporation, San Jose, CA) and frame-grabber software (Mediacruise, Canopus Corporation, San Jose, CA). The cine-clips were subsequently stored on digital video discs (DVDs) after the end of the ultrasound examination.

CT examination

CT of the liver was performed with 64-row multi-detector CT systems [Aquilion, Toshiba, Tokio, JA (n=71 patients); Brilliance, Philips, Cleveland, OH (n=35)]. Patients were instructed to hold their breath with tidal inspiration during scanning. Technical parameters were: rotation time, 400 ms; beam collimation, 64×0.5 mm (Aquilion, Toshiba), 64×0.625 mm (Brilliance, Philips); normalized pitch, 1; z-axis coverage, 32 mm; reconstruction interval, 0.3-mm; tube voltage, 120-kV; tube current (effective mAs), 180–250 mAs depending on patient size, and field of view, 40 cm. Image reconstruction was performed in a 25–35-cm display field of view, depending on the patient's physique. Studies consisted of an unenhanced CT acquisition, followed by arterial, portal venous, and delayed equilibrium phases acquired after the i.v. bolus injection of iodinated contrast material (Iomeron 400, Bracco, Milan, Italy; 400 mg I/ml, 5 ml/s at 2 ml/kg followed by 50 ml of saline flush) administered with a dual-syringe power injector (Stellant CT injector, Medrad, Indianola, PA) via a 20-gauge catheter inserted into an antecubital vein. An automatic bolus-tracking program (Bolus Pro Ultra; Philips Medical Systems) was used to time the start of arterial phase scanning after contrast material injection. The CT number was monitored by one region-of-interest (ROI) cursor (0.8–2.0 cm²) placed in the abdominal aorta at the L1 vertebral body level with a trigger threshold set at 140 HU. The arterial phase started with a delay of 18 s after the threshold had been reached [20]. Real-time, low-dose (120 kVp, 15 mAs) serial monitoring studies began 8 s after the start of the contrast material injection. The portal venous phase was initiated at about 70–80 s after the start

Table 2 Analysis of nodule vascularity during the arterial phase – reader 1

Histotypes	CEUS		CT	
	Hypervascular	Iso- or hypovascular	Hypervascular	Iso- or hypovascular
Hepatocellular carcinomas	64	8	52	20
Dysplastic nodules	2	8	2	8
Regenerative nodules	3	12	0	15
Hemangiomas	3	9	3	9
Other benign histotypes	2	1	2	1
Pseudotumors	3	6	4	5
Total	77	44	63	58

Table 3 Analysis of nodule vascularity during the arterial phase – reader 2

Histotypes	CEUS		CT	
	Hypervascular	Iso- or hypovascular	Hypervascular	Iso- or hypovascular
Hepatocellular carcinomas	63	9	51	21
Dysplastic nodules	5	5	2	8
Regenerative nodules	1	14	0	15
Hemangiomas	3	9	3	9
Other benign histotypes	2	1	2	1
Pseudotumors	4	5	4	5
Total	78	43	62	59

of contrast injection and the delayed equilibrium phase at about 180–210 s after the start of injection of contrast agent.

Hepatocellular nodules biopsy

Within 15 days after CT, the percutaneous US-guided biopsy was performed with 18-20-gauge modified Menghini needles and stained with hematoxylin/eosin and the Masson trichrome method. A senior pathologist for each center made the diagnosis according to the diagnostic criteria established by the International Working Party on the terminology of nodular hepatocellular lesions [1].

Independent analysis of nodule vascularity and cine-clip interpretation

The CEUS and MDCT examinations were reviewed independently by two radiologists with 2 and 8 years of experience in liver imaging who were blinded to the patients' identification, clinical histories, biopsy results, and other imaging findings. CEUS digital cine-clips were randomly assigned to each reader, and all readings were performed on the same computer (Intel, Pentium 4 with 19-inch TFT display, resolution 2,560×1,600 pixels, Santa Clara, CA) by using Power-DVD software (CyberLink Corporation, Fremont, CA). Readers were free to perform real-time scrolling of the digital cine-clips. Two weeks later CT images were randomly assigned to each reader, and all readings were performed on a Picture Archiving and Communications System (PACS), integrated workstation (19-inch TFT display, resolution 2,560×1,600 pixels, Ebit Sanità AET, Genoa, Italy) at a central location. Readers scrolled the CT images during arterial, portal, and delayed phase and were free to change the window level and the window width. Transverse sections and multiplanar reformations were used for image display.

Uniform criteria were adopted to define nodule vascularity on CEUS and CT analysis. Nodules displaying higher, similar, or lower enhancement compared to the adjacent liver parenchyma (within 3 cm from the outer nodule border) were defined as hyper-, iso-, or hypovascular, respectively. Hypervascularity could be homogeneously or heterogeneously distributed throughout the nodule. Nodules with dot-like vascularity (tiny separate spots of enhancement) were considered hypovascular. Evidence of rim-like vascularity (continuous peripheral ring) was recorded. For consistency in the analysis, the portal venous and delayed phases were analyzed in combination (e.g., nodules appearing isovascular in the portal phase and hypovascular in the delayed phase were classified as hypovascular). Immediately after analysis of the CT images, combined CEUS/CT examinations were evaluated side by side by each reader. Concordant vascular profiles on CEUS and CT were not

Table 4 Analysis of nodule vascularity during the portal and delayed phase – reader 1

Histotypes	CEUS		CT	
	Hyper- or isovascular	Hypovascular	Hyper- or isovascular	Hypovascular
Hepatocellular carcinomas	39	33	15	57
Dysplastic nodules	10	0	10	0
Regenerative nodules	15	0	14	1
Hemangiomas	11	1	11	1
Other benign histotypes	2	1	2	1
Pseudotumors	9	0	9	0
Total	86	35	61	60

Table 5 Analysis of nodule vascularity during the portal and delayed phase – reader 2

Histotypes	CEUS		CT	
	Hypovascular	Hyper- or isovascular	Hypovascular	Hyper- or isovascular
Hepatocellular carcinomas	38	34	15	57
Dysplastic nodules	10	0	10	0
Regenerative nodules	15	0	14	1
Hemangiomas	11	1	10	2
Other benign histotypes	2	1	2	1
Pseudotumors	9	0	9	0
Total	85	36	60	61

The hepatocellular nodule vascular profiles on contrast-enhanced US (CEUS) and 64-row multidetector CT (CT)

Fig. 1 Well-differentiated hepatocellular carcinoma (1.5 cm) in a 46-year-old man with liver cirrhosis related to virus C infection. Concordance between contrast-enhanced US and 64-ro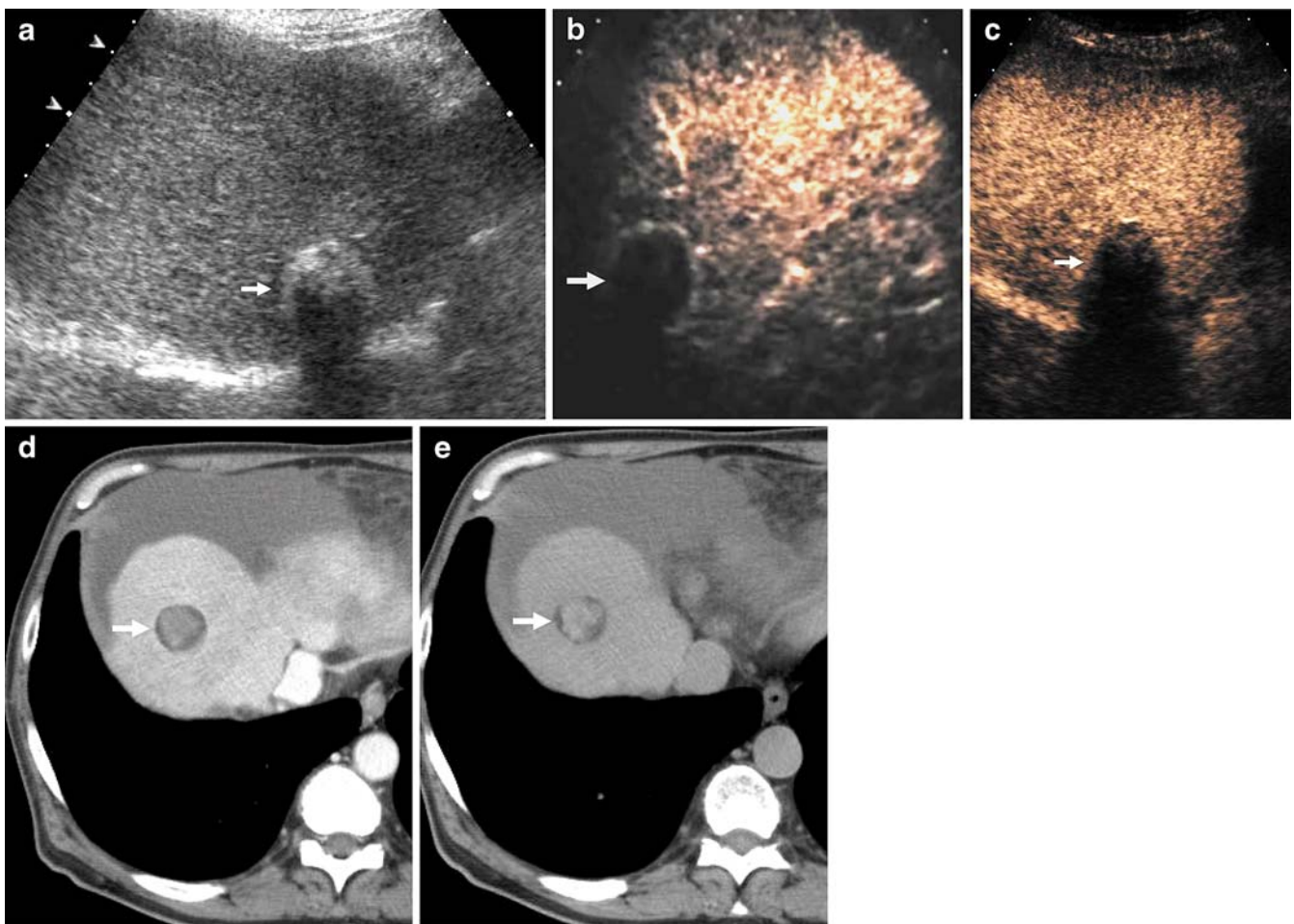w multi-detector CT. (a, b) Contrast-enhanced US. Transverse image of the right lobe of the liver. The nodule (arrow) appears homogeneously hypervascular during the arterial phase (a) and slightly hypervascular in comparison to the adjacent liver parenchyma during the portal venous phase (b). (c, d) Transverse CT scan of the right lobe of the liver. The same pattern of vascularity is observed at mulidetector CT during the arterial (c) and portal venous phase (d). Both readers correctly considered the nodule malignant (diagnostic confidence level=4) after the analysis of contrast-enhanced US, CT, and combined contrast-enhanced US/CT
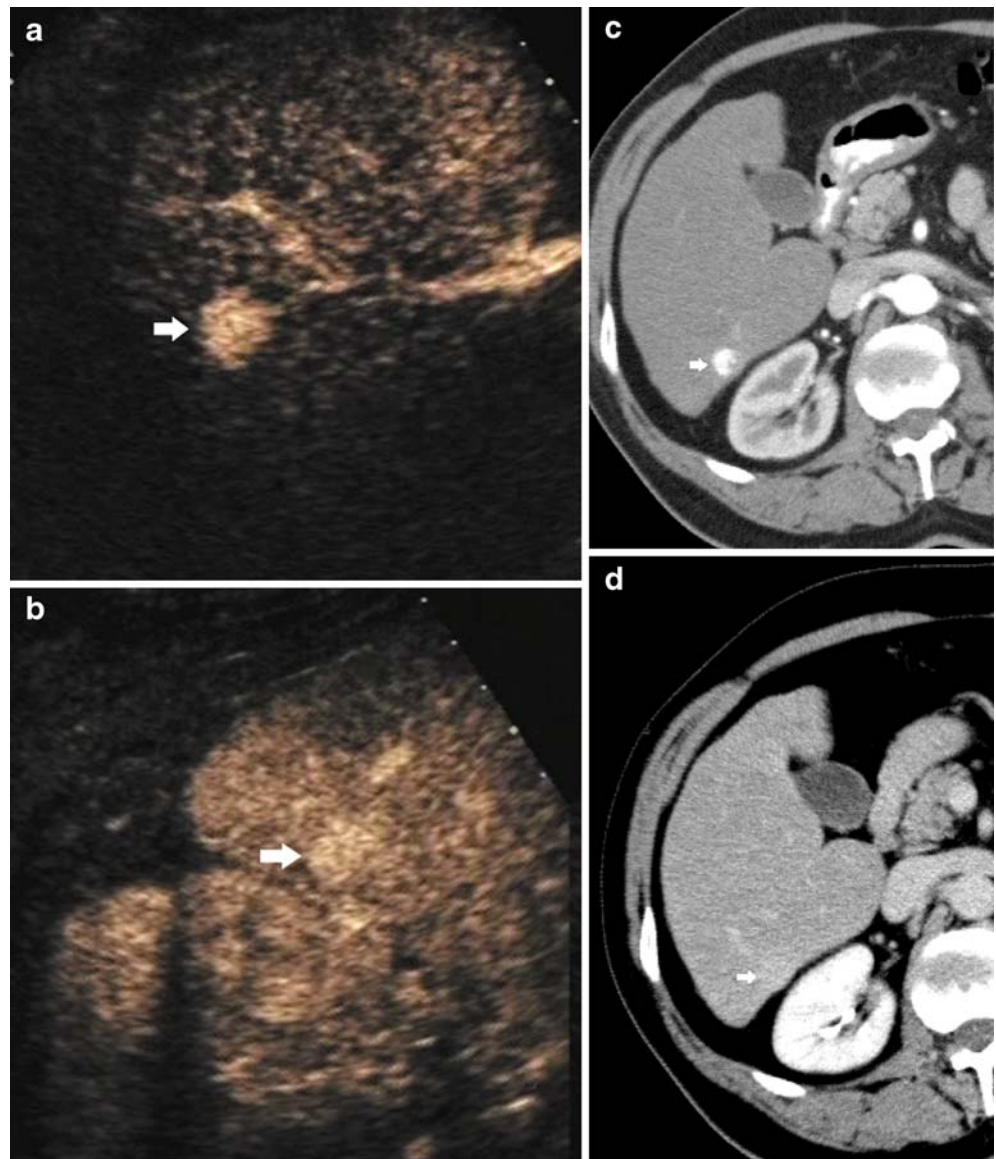
required for the purposes of the study, and the higher grade of vascularity observed during the arterial phase was considered decisive (e.g., nodules appearing hypervascular on CEUS and isovascular on CT were classified as hypervascular). In nodules appearing hypervascular during the arterial phase, the lower grade of vascularity in the portal/delayed phase was considered decisive (e.g., hypervascular nodules appearing isovascular on CEUS and hypovascular on CT during the portal/delayed phase were classified as hypovascular).

In each reading session, both readers expressed diagnostic confidence on a five-level scale: (1) definitely benign (nodules appearing persistently isovascular or also nodules with peripheral nodular vascularity with centripetal fill-in); (2) probably benign (nodules appearing hypovascular during the arterial phase and isovascular during the portal and delayed phase); (3) indeterminate (nodules appearing persistently hypovascular or nodules appearing isovascular during the arterial phase and hypovascular during the portal and delayed phase); (4) probably malignant (nodules appearing hypervascular during the arterial phase and iso- or hypervascular during the portal and delayed phase or nodules appearing persistently hypovascular with evidence of peripheral rim-like enhancement); (5) definitely malignant (nodules appearing hypervascular during the arterial phase and hypovascular during the portal and delayed phase with or without peripheral vascular rim).

Fig. 2 Well-differentiated hepatocellular carcinoma (2 cm) in a 75-year-old man with liver cirrhosis related to virus B infection. Concordance between contrast-enhanced US and 64-row multi-detector CT. (a) Unenhanced US. Transverse image of the right lobe of the liver. A hypoechoic nodule (arrow) with posterior acoustic shadowing is evident near the diaphragm. (b, c) Contrast-enhanced US. The nodule appears hypovascular both during the arterial (b) and portal venous phase (c). (d, e) Transverse CT scan of the right lobe of the liver. The same nodule appears hypovascular during the arterial (d) and portal venous phase also with evidence of a peripheral hyperdense rim (e). The nodule was correctly considered malignant (diagnostic confidence level=4) by the second reader after evaluation of CT and combined contrast-enhanced US/CT images due to the peripheral hyperdense rim, whereas the same nodule was interpreted as indeterminate (diagnostic confidence level= 3) by the first reader

Statistical analysis

A biostatistician participated in the statistical analysis performed by a computer software package (Analyse-it, version 1.63, Analyse-it-software, Leeds, UK). Retrospective benign or malignant diagnosis was considered as true positive (lesion correctly assessed as malignant, confidence levels 4 or 5), false negative (malignant lesions incorrectly assessed as benign, confidence levels 1, 2, or assessed as indeterminate, confidence level 3), true negative (lesion correctly assessed as benign, confidence levels 1, 2), or false positive (benign lesions incorrectly assessed as malignant, confidence levels 4 or 5, or assessed as indeterminate, confidence level 3). The McNemar test was used to compare the sensitivity and specificity of unenhanced US and CEUS, whereas improvement in diagnostic confidence was assessed by ROC curve analysis by plotting the sensitivity (true-positive fraction) against 1-specificity (false-positive fraction). The area under each ROC curve was calculated by using a non-parametric method [21], and the method proposed by Hanley and McNeil [22] was employed to compare areas under each ROC curve. A P value<0.05 was considered to indicate a statistically significant difference.

Weighted k statistics were calculated to assess inter-reader agreement in the visual analysis. Agreement was graded as poor (k value<0.20), moderate (≥0.20 and <0.40), fair (≥0.40 and <0.60), good (≥0.60 and <0.80), and very good (≥0.8-1).

Results

Tables 2, 3, 4, and 5 show the different vascularity profiles observed in the different histotypes according to reader 1
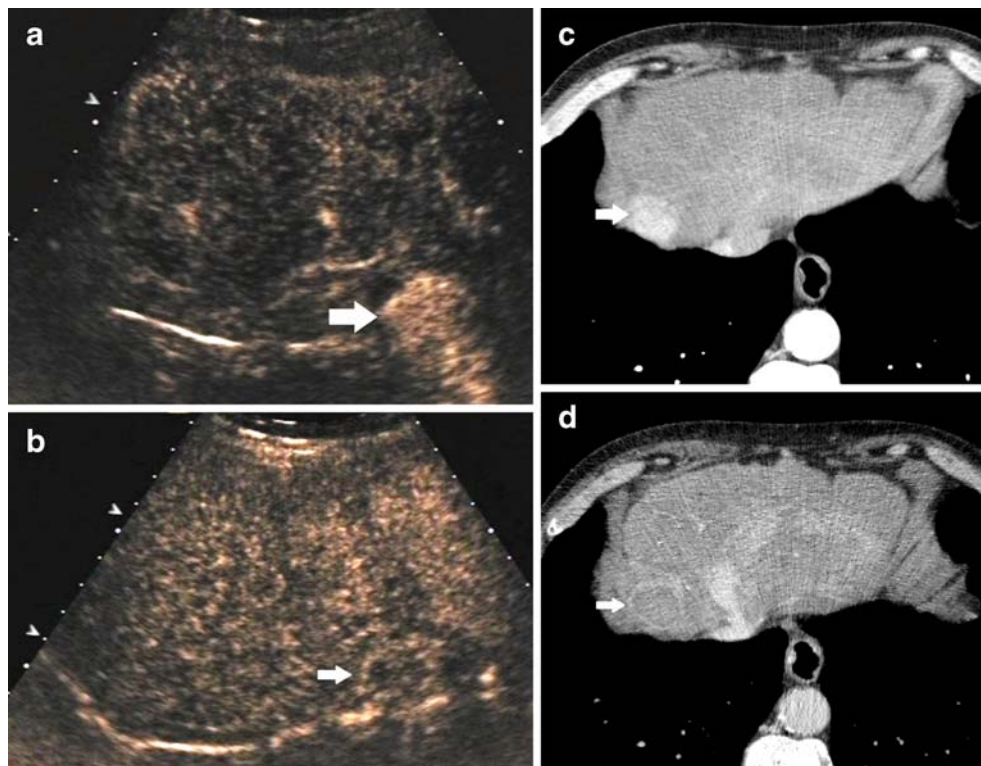

Fig. 3 Well–differentiated hepatocellular carcinoma (15 mm) in a 56-year-old woman with liver cirrhosis related to virus C infection. Discordance between contrast-enhanced US and 64-row multi-detector CT during the arterial phase. (a, b) Contrast-enhanced US. The nodule (arrow) appears isovascular to the adjacent liver parenchyma both during the arterial (a) and the portal venous phase (b). (c, d) Transverse CT scan of the right lobe of the liver. The nodule appears hypervascular during the arterial phase (c) and slightly hypervascular during the portal venous phase (d). Both readers considered the nodule benign (diagnostic confidence level=1) after the analysis of contrast-enhanced US, while they correctly classified the nodule as malignant (diagnostic confidence level=4) after CT and combined contrast-enhanced US/CT analysis
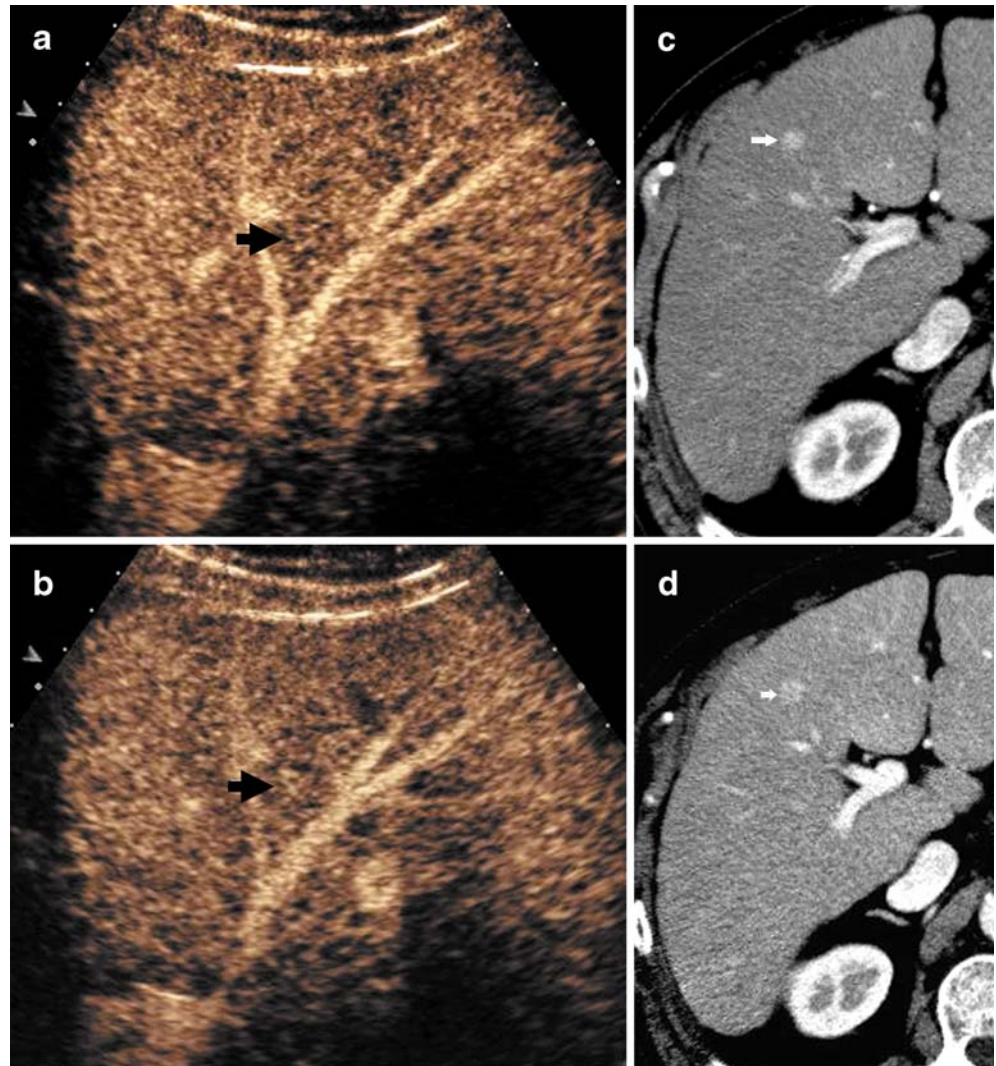
and 2. A concordant vascularity profile on CEUS and CT (Figs. 1 and 2) was observed in the majority of hepatocellular nodules, whereas discordant vascularity profiles were observed in a limited number of nodules (Figs. 3, 4, 5, and 6). Discordance between CEUS and CT in depicting hepatocellular nodule vascularity during the arterial phase was observed in 16/121 hepatocellular nodules (≤2 cm, 14 nodules, or >2 cm, 2 nodules), including 12 HCCs (according to both readers), 3 regenerative nodules, and 1 pseudotumor (according to reader 1) or 1 regenerative nodule and 3 dysplastic nodules (reader 2). Those hepatocellular nodules appearing isovascular on CEUS and hypervascular on CT during the arterial phase (n=2 nodules according to both readers) had deep locations in the liver near the diaphragm or the heart (Fig. 3). Those hepatocellular nodules appearing hypervascular on CEUS and iso- or hypovascular on CT during the arterial phase

(n=16 nodules according to both readers) were located in the anterior segments of the liver (Fig. 5).

Tables 6 and 7 show the diagnostic performance and confidence of the two readers for CEUS, CT, and combined CEUS/CT analysis, respectively. The evaluation of CEUS provided 8 (according to reader 1) or 9 (reader 2) false-negative findings, and 15 (according to reader 1) or 18 (reader 2) false-positive findings. The evaluation of CT provided 19 (according to reader 1) or 21 (reader 2) false-negative findings and 14 (both readers) false-positive findings. False-negative findings corresponded to HCCs appearing iso- or hypovascular during the arterial phase and isovascular in the portal and delayed phase and interpreted as benignancies, or persistently hypovascular HCCs that were considered indeterminate on both CEUS and CT. False-positive findings corresponded to dysplastic nodules and hyper-


Fig. 4 Well-differentiated hepatocellular carcinoma (2.5 cm) in a 53-year-old man with liver cirrhosis related to virus B infection. Discordance between contrast-enhanced US and 64-row multidetector CT during the portal venous phase. (a, b) Contrast-enhanced US. Transverse image of the right lobe of the liver. The nodule (arrow) appears homogeneously hypervascular during the arterial phase 25 s after microbubble injection (a) and hypovascular in comparison to the adjacent liver parenchyma during the portal venous phase 80 s after microbubble injection (b), also with evidence of peripheral vascular rim. (c, d) Transverse CT scan of the right lobe of the liver. The same pattern of vascularity is observed at CT during the arterial phase (c), while the nodule appears isovascular to the adjacent liver with evidence of peripheral rim during the portal venous phase (d). Both readers correctly considered the nodule malignant (diagnostic confidence level=4) after the analysis of CT, even though they were more confident after contrast-enhanced US and combined contrast-enhanced US/CT analysis (diagnostic confidence level=5) due to nodule hypovascularity during the portal venous phase after microbubble contrast agent injection

Fig. 5 Low-grade dysplastic nodule (1 cm) in a 42-year-old man with liver cirrhosis related to virus B infection. Discordance between contrast-enhanced US and 64-row multi-detector CT during the arterial phase. (a, b) Contrast-enhanced US. Transverse image of the right lobe of the liver. The nodule (arrow) appears homogeneously hypervascular 35 s after microbubble injection during the arterial phase (a). Evidence of nodule isovascularity to the adjacent liver during the portal venous phase 80 s after microbubble injection (b). (c, d) Transverse CT scan of the right lobe of the liver. The same nodule (arrow) appears isovascular on CT during the arterial (c) and portal venous phase (d). The nodule was misinterpreted as malignant by both readers after the contrast-enhanced US and combined contrast-enhanced US/CT analysis (diagnostic confidence level=4) due to the nodule hypervascularity during the arterial phase after microbubble contrast agent injection
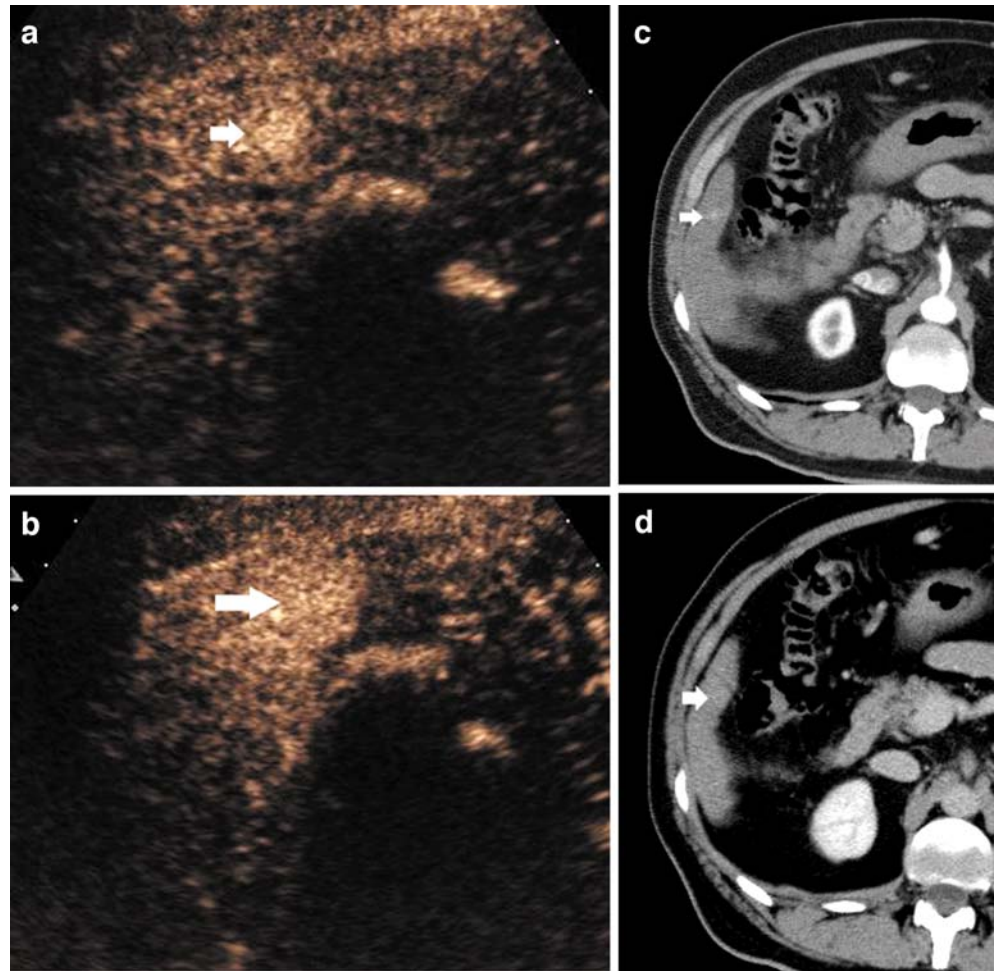
vascular benignancies that appeared hypervascular during the arterial phase and hypo- or isovascular in the portal venous and delayed phase. The combined CEUS/CT analysis produced two false-negative findings (according to both readers) corresponding to HCCs that appeared persistently hypovascular at both CEUS and CT (Fig. 2). Despite the reduction in the false-negative findings, the combined CEUS/CT analysis produced 14 (according to reader 1) or 15 (reader 2) false-positive findings corresponding to hypervascular benignancies that appeared hypervascular during the arterial phase and isovascular in the portal venous and delayed phase at both CEUS and CT (Fig. 5).

The analysis of the arterial phase produced a good inter-reader agreement for CEUS and CT (k value=0.7 and 0.75) and very good agreement for combined CEUS/CT (k value=0.9). The analysis of the portal phase produced a very good inter-reader agreement for both CEUS and CT (k value=0.85 and 0.90) and for combined CEUS/CT (k value=0.95). The ROC analysis (Fig. 7) revealed a clear-cut increase in diagnostic confidence at the combined CEUS/CT analysis.

Discussion

This retrospective study was performed to analyze the potential added diagnostic performance of combined CEUS and 64-row multidetector CT in the characterization of hepatocellular nodules in cirrhotic patients. In our study the combined assessment of CEUS and CT improved diagnostic accuracy in the diagnosis of malignancy. This study confirms the results of previous studies [13–15] revealing the general concordance of CEUS with CT in depicting arterial hypervascularity in the majority of hepatocellular nodules and particularly in HCCs. The level of discordance between CEUS and CT in depicting hepatocellular nodule vascularity in cirrhotic patients was
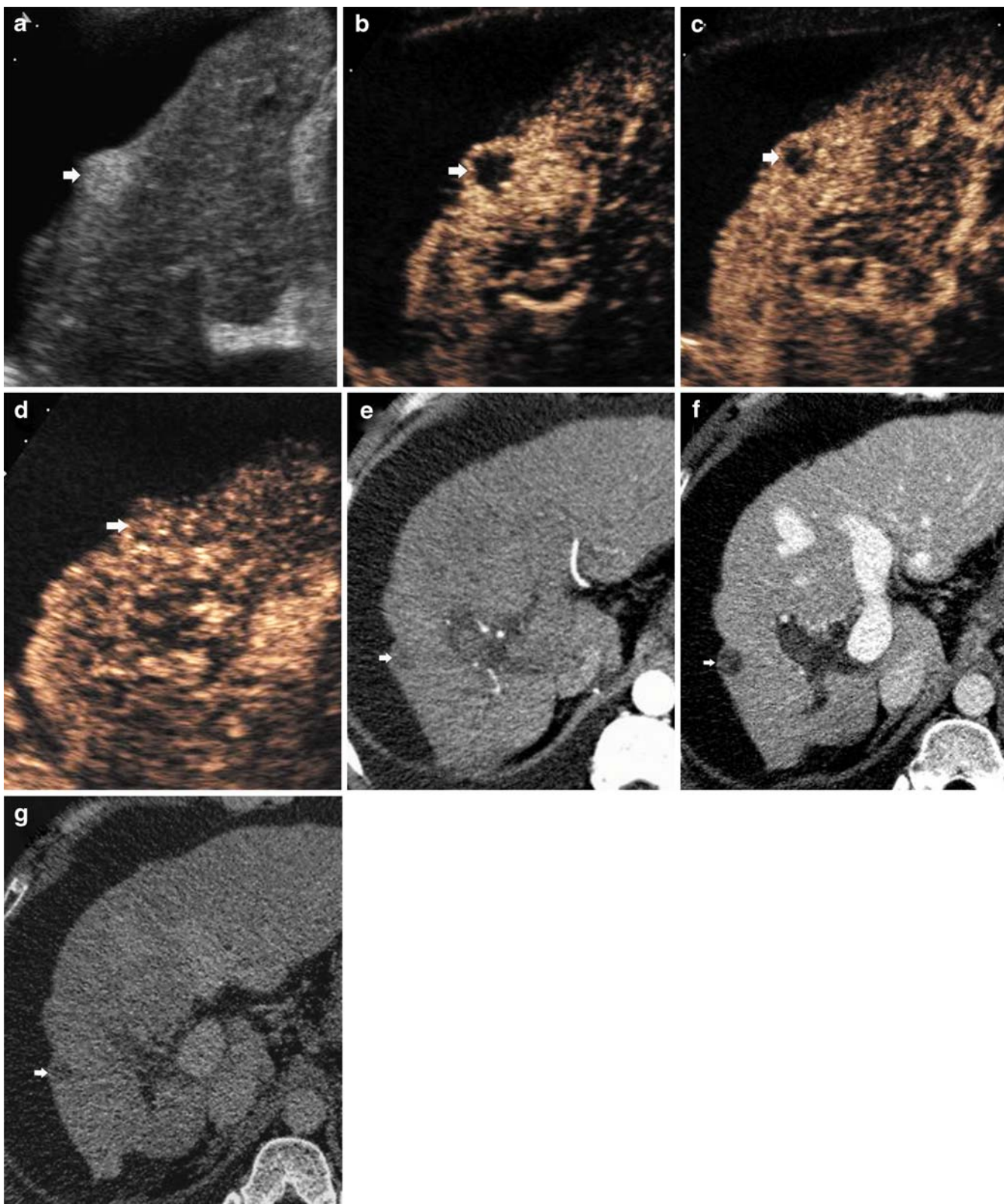
Fig. 6 Regenerative nodule (15 mm) in a 57-year-old man with liver cirrhosis related to virus C infection. Discordance between contrast-enhanced US and 64-row multi-detector row CT during the portal venous phase. (a) Unenhanced US, longitudinal scan. The nodule (arrow) is hyperechoic and located near the hepatic dome. (b - d) Contrast-enhanced US. Longitudinal image of the right lobe of the liver. The nodule appears hypovascular 35 s after microbubble injection during the arterial phase (b) and 60 s after microbubble injection during the portal venous phase (c). Evidence of nodule isovascularity to the adjacent liver during the delayed sinusoidal phase 160 s after microbubble injection (d). (e-g) Transverse CT scan of the right lobe of the liver. The nodule appears hypovascular on multidetector CT during the arterial (e) and portal venous phase (f) and also on the delayed phase (g). The nodule was correctly interpreted as benign by both readers (diagnostic confidence level=2) after the contrast-enhanced US and combined contrast-enhanced US/CT analysis based on the isovascularity evident on contrast-enhanced US during the delayed sinusoidal phase, while the same nodule was considered indeterminate (diagnostic confidence level=3) after CT analysis

Table 7 Independent cine-clip interpretation - reader 2

Reader 2	CEUS	CT	CEUS and CT
Sensitivity	87 (63/72)	71 (51/72)	97 (70/72)
Specificity	63 (31/49)	71 (35/49)	69 (34/49)
PPV	77 (63/81)	78 (51/65)	82 (70/85)
NPV	77 (31/40)	62 (35/56)	94 (34/36)
Accuracy	77 (94/121)	71 (86/121)	85 (104/121)
Confidence *	0.876	0.892	0.960
	(0.815 – 0.937)	(0.835 – 0.949)	(0.932 – 0.988)

Independent analysis. Sensitivity, specificity, positive predictive value (PPV), negative predictive value (NPV), and accuracy after review of contrast-enhanced US (CEUS), multidetector CT (CT), and combined CEUS and CT for reader 1 (a) and reader 2 (b). Numbers are expressed as percentages, and the numbers from which percentages were calculated are reported in brackets, except for diagnostic confidence (*) expressed as areas - A_z - under the ROC curves where numbers are real values with 95% confidential values between brackets. All differences among CEUS, CT, and combined CEUS and CT were statistically significant (P<0.05).

reported as 19%, and 22% in hepatocellular nodules <2 cm [14]. In our study the lower level of discordance between CEUS and CT during the arterial phase was probably due to the greater capability of 64-row multidetector CT in depicting nodule vascularity. A higher level of discordance was observed in the portal venous phase, which may reflect the tendency of CT and MR contrast agents, unlike microbubbles, to diffuse into interstitium.

In our study the most important improvement in diagnosis provided by the combined assessment of CEUS/CT was the reduction of false-negative findings. This means that HCCs are more correctly characterized by the combination of the two techniques than by the separate techniques. Most HCCs that appeared persistently isovascular at CEUS or CT were correctly interpreted at combined CEUS and CT since they revealed unequivocal hypervascularity during the arterial phase and/or hypovas-cularity during the portal venous phase. Evidence of hypovascularity in the portal venous phase was considered as a supportive feature in the diagnosis of malignancy, whereas evidence of isovascularity in the portal venous phase in nodules appearing hypervascular during the arterial phase did not exclude malignancy. This was due to the diagnostic criteria adopted in the present study, which were derived from the 2001 Barcelona criteria [2, 3] that considered hepatocellular nodule hypervascularity during the arterial phase as the principal landmark for a diagnosis of malignancy. Concordant findings on CEUS and CT were not requested in our study, and the combined assessment was performed to increase the diagnostic accuracy of each technique. In a few nodules some technical difficulties due to US beam attenuation (nodules near the diaphragm or the heart) limited the visibility of nodule enhancement after microbubble injection. This observation is in agreement with a previous study in which 7% of 60 HCCs scanned after air-filled microbubble injection displayed no vascular signal because of their deep location [23].

In our series several benign hepatocellular nodules revealed arterial-phase hypervascularity on both CEUS and CT and were incorrectly interpreted as malignancies. In fact, despite the reduction in false-negative findings, there were a persisting number of false-positive findings, i.e., hypervascular benign lesions considered malignant (14 reader 1 and 15 reader 2, out of 120) even after combined CEUS/CT interpretation. This confirms the results of

Table 6 Independent cine-clip interpretation - reader 1

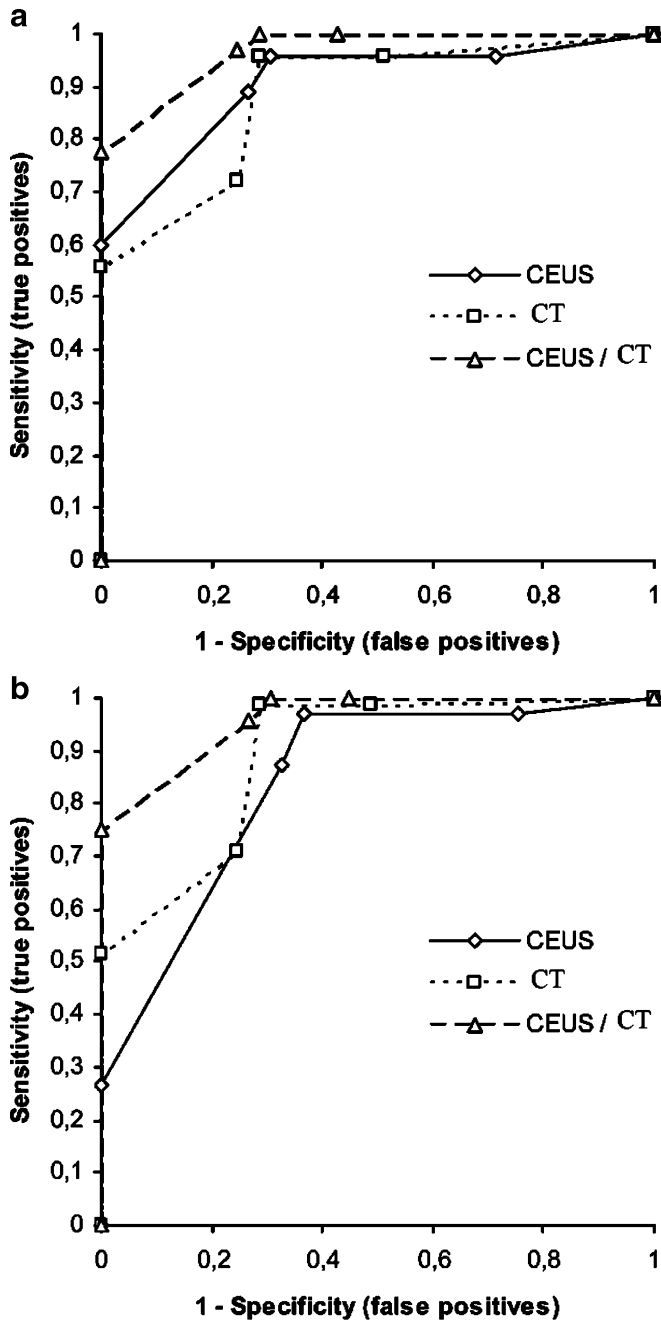| Reader 1	CEUS	CT	CEUS and CT
Sensitivity	88 (64/72)	74 (53/72)	97 (70/72)
Specificity	69 (34/49)	71 (35/49)	71 (35/49)
PPV	81 (64/79)	79 (53/67)	83 (70/84)
NPV	80 (34/42)	64 (35/54)	94 (35/37)
Accuracy	80 (98/121)	72 (88/121)	86 (105/121)
Confidence *	0.906	0.885	0.969
	(0.853 – 0.959)	(0.827 – 0.944)	(0.945 – 0.993)

Fig. 7 (a, b) Receiver operating characteristic (ROC) analysis for the first reader (2 years of experience) (a) and the second reader (8 years of experience) (b). CEUS = Contrast- enhanced US. CT = Mulidetector CT

appeared iso- or hypovascular in the arterial phase and isovascular in the portal venous phase because of the prevalent portal blood supply and were correctly interpreted as benign. However, those benign nodules appearing iso- or hypervascular in the arterial phase and hypovascular in the portal venous phase were misclassifed as malignant. CEUS may potentially further increase the percentage of benign nodules appearing hypervascular in the arterial phase, owing to the very high sensitivity of contrast-specific US techniques to the harmonic signals produced by microbubble insonation and may increase the number of benign nodules deemed malignant undergoing biopsy or interventional procedures with potential morbidity and incremental costs. On the other hand, this study showed that CEUS presents some clear limitations in depicting hepatocellular nodule vascularity in those hepatocellular nodules with a deep location in the liver, which limits the visibility of the nodule enhancement after microbubble injection due to echo-signal attenuation [23].

The diagnostic performance and confidence of independent analysis revealed a very high inter-reader agreement, even though the readers had different levels of experience. This result is explained by the characteristic vascular patterns observed in most nodules both at CEUS and at CT. However, an inevitable inter-reader variability accounts for the difference in diagnostic performance and confidence.

According to the results of the present study, CEUS should be considered a preliminary examination after unenhanced US to exclude malignancy and a reliable additional imaging technique to CT or MR imaging for characterizing those hepatocellular nodules detected during US surveillance given that the diagnostic criteria developed for CEUS are similar to those proposed by the Barcelona committee for CT and MR imaging [2, 3]. When a typical enhancement pattern is identified (hypervascularity during the arterial phase and hypovascularity in the portal venous phase, or hyper- or isovascularity during the arterial phase and isovascularity in the portal venous phase in nodules >2 cm), these diagnostic criteria allow the characterization of most malignant hepatocellular nodules. At CT proper timing of the arterial phase is crucial to identify hypervascular nodules and requires the use of a test dose injection or a bolus tracking system to initiate scanning at an optimal phase of opacification. MR imaging [30, 31], also with the use of liver-specific contrast agents (including hepatocyte-targeted agents and reticuloendothelial system-targeted agents), may be useful to clarify questionable cases owing to the ability to show the changes in hepatobiliary function or Kuppfer cell content associated with malignancy. The principal limitation of this study is represented by the strict inclusion criteria, which led to the exclusion of a significant number of nodules without a histological diagnosis.

In conclusion, the combined assessment of hepatocellular nodule vascularity at multiphasic 64-row multidetector CT and CEUS improved sensitivity in the diagnosis of malignancy in patients with liver cirrhosis.

previous studies [24–28] that have shown that a large portion of the false-positive diagnoses of HCC are due to enhancing benign lesions and that the use of a suspicious pattern only (arterial contrast uptake regardless of washout) increases the number of false positives compared with the use of conclusive definitions (arterial uptake followed by washout) [29]. Most regenerative and dysplastic nodules

References

1. International Working Party (1995) Terminology of nodular hepatocellular lesions. Hepatology 22:983–993
2. Bruix J, Sherman M, Llovet JM et al (2001) Clinical management of hepatocellular carcinoma. Conclusions of the Barcelona-2000 EASL conference. European Association for the Study of the Liver. J Hepatol 35:421–430
3. Bruix J, Sherman M (2005) Management of hepatocellular carcinoma. Hepatology 42:1208–1236
4. Iannacone R, Laghi A, Catalano C et al (2004) Focal liver lesions in the cirrhotic patient: multislice spiral CT evaluation. Radiol Med 107:304–316
5. Laghi A, Iannacone R, Rossi P et al (2003) Hepatocellular carcinoma: detection with triple-phase multi-detector row helical CT in patients with chronic hepatitis. Radiology 226:543–549
6. Ichikawa T, Kakajima H, Nanbu A, Hori M, Araki T (2006) Effect of injection rate of contrast material on CT of hepatocellular carcinoma. AJR Am J Roentgenol 186:1413–1418
7. Monzawa S, Ichikawa T, Nakajima H, Kitanaka Y, Omata K, Araki T (2007) Dynamic CT for detecting small hepatocellular carcinoma: usefulness of delayed phase imaging. AJR Am J Roentgenol 188:147–153
8. Claudon M, Cosgrove D, Albrecht T et al (2008) Guidelines and good clinical practice recommendations for contrast enhanced ultrasound (CEUS)–Update 2008. Ultraschall Med 29:28–44
9. Quaia E, Calliada F, Bertolotto M, Rossi S, Garioni L, Rosa L, Pozzi-Mucelli R (2004) Characterization of focal liver lesions by contrast-specific US modes and a sulfur hexafluoride-filled microbubble contrast agent: diagnostic performance and confidence. Radiology 232:420–430
10. Nicolau C, Catalá V, Vilana R, Gilabert R, Bianchi L, Sole M, Pages M, Bru C (2004) Evaluation of hepatocellular carcinoma using SonoVue, a second generation ultrasound contrast agent: correlation with cellular differentiation. Eur Radiol 14:1092–1099
11. Giorgio A, Ferraioli G, Tarantino L et al (2004) Contrast-enhanced sonographic appearance of hepatocellular carcinoma in patients with cirrhosis: Comparison with contrast-enhanced CT appearance. AJR Am J Roentgenol 183:1319–1326
12. Quaia E, D'Onofrio M, Cabassa P et al (2007) Diagnostic value of hepatocellular nodule vascularity after sulfur hexafluoride-filled microbubble injection in patients with liver cirrhosis: analysis of diagnostic performance and confidence in malignancy characterization. AJR Am J Roentgenology 189:1474–1483
13. Gaiani S, Celli N, Piscaglia F et al (2004) Usefulness of contrast-enhanced perfusional sonography in the assessment of hepatocellular carcinoma hypervascular at spiral computed tomography. J Hepatol 41:421–426
14. Bolondi L, Gaiani S, Celli N et al (2005) Characterization of hepatocellular nodules in 40 cirrhosis by assessment of vascularity: the problem of hypovascular hepatocellular carcinoma. Hepatology 42:27–34
15. Pompili M, Riccardi L, Semeraro S et al (2008) Contrast-enhanced ultrasound assessment of arterial vascularization of small nodules arising in the cirrhotic liver. Dig Liver Dis 40 (3):206–215
16. Burns P, Wilson SR (2007) Focal liver lesions: enhancement patterns on contrast-enhanced images – Concordance of US scans with CT scans and MR images. Radiology 242(1):162–174
17. Forner A, Villana R, Ayuso C et al (2008) Diagnosis of hepatic nodules 20 mm or smaller in cirrhosis: prospective validation of the noninvasive diagnostic criteria for hepatocellular carcinoma. Hepatology 47:97–104
18. Bismuth H (1982) Surgical anatomy and anatomical surgery of the liver. World J Surg 6:3–8
19. Couinaud C (1957) Le foie: études anatomiques et chirurgicales. Masson, Paris, pp 9–12
20. Sultana S, Awai K, Nakayama Y et al (2007) Hypervascular hepatocellular carcinomas: bolus tracking with a 40-detector CT scanner to time arterial phase imaging. Radiology 243:140–147
21. Beck JR, Shultz EK (1986) The use of relative operating characteristic (ROC) curves in test performance evaluation. Arch Pathol Lab Med 110:13–20
22. Hanley JA, McNeil BJ (1983) A method of comparing the areas under receiver operating characteristic curves derived from the same cases. Radiology 148:839–843
23. Tanaka S, Ioka T, Oshikawa O, Hamada Y, Yoshioka F (2001) Dynamic sonography of hepatic tumours. AJR Am J Roentgenol 177:799–805
24. Lee HM, Lu DS, Krasny RM, Busuttil R, Kadell B, Lucas J (1997) Hepatic lesion characterization in cirrhosis: significance of arterial hypervascularity on dual-phase helical CT. AJR Am J Roentgenol 169:125–130
25. Baron RL, Peterson MS (2001) Screening the cirrhotic liver for hepatocellular carcinoma with CT and MR imaging: opportunities and pitfalls. Radiographics 21:S117–S132
26. Lim JH, Kim CK, Lee WJ et al (2000) Detection of hepatocellular carcinomas and dysplastic nodules in cirrhotic livers: accuracy of helical CT in transplant patients. AJR Am J Roentgenol 175:693–698
27. Rode A, Bancel B, Douek P et al (2001) Small nodule detection in cirrhotic livers: evaluation with US, spiral CT, and MRI and correlation with pathologic examination of explanted liver. J Comput Assist Tomogr 25(3):327–336
28. Valls C, Cos M, Figueras J et al (2004) Pretransplantation diagnosis and staging of hepatocellular carcinoma in patients with cirrhosis: value of dual phase helical CT. AJR Am J Roentgenol 182:1011–1017
29. Forner A, Vilana R, Ayuso C et al (2007) Diagnosis of hepatic nodules 20 mm or smaller in cirrhosis: prospective validation of the noninvasive diagnostic criteria for hepatocellular carcinoma. Hepatology 47:1–7
30. Krinsky GA, Lee VS, Theise ND et al (2001) Hepatocellular carcinoma and dysplastic nodules in patients with cirrhosis: prospective diagnosis with MR imaging and explantation correlation. Radiology 219:445–454
31. Bhartia B, Ward J, Guthrie JA, Robinson PJ (2003) Hepatocellular carcinoma in cirrhotic livers: double-contrast thin-section MR imaging with pathologic correlation of explanted tissue. AJR Am J Roentgenol 180:577–584